Physical Biology

PAPER

Morphogen-regulated contact-mediated signaling between cells can drive the transitions underlying body segmentation in vertebrates

RECEIVED
4 June 2021

REVISED
13 October 2021

ACCEPTED FOR PUBLICATION
20 October 2021

PUBLISHED
11 November 2021

Chandrashekar Kuyyamudi[1,2], Shakti N Menon[1] and Sitabhra Sinha[1,2,*]

[1] The Institute of Mathematical Sciences, CIT Campus, Taramani, Chennai 600113, India
[2] Homi Bhabha National Institute, Anushaktinagar, Mumbai 400 094, India
[*] Author to whom any correspondence should be addressed.

E-mail: sitabhra@imsc.res.in

Keywords: somitogenesis, morphogen gradients, notch-delta signaling, genetic oscillator, clock and wavefront mechanism, segmentation

Supplementary material for this article is available online

Abstract

We propose a unified mechanism that reproduces the sequence of dynamical transitions observed during somitogenesis, the process of body segmentation during embryonic development, that is invariant across all vertebrate species. This is achieved by combining inter-cellular interactions mediated via receptor-ligand coupling with global spatial heterogeneity introduced through a morphogen gradient known to occur along the anteroposterior axis. Our model reproduces synchronized oscillations in the gene expression in cells at the anterior of the presomitic mesoderm as it grows by adding new cells at its posterior, followed by travelling waves and subsequent arrest of activity, with the eventual appearance of somite-like patterns. This framework integrates a boundary-organized pattern formation mechanism, which uses positional information provided by a morphogen gradient, with the coupling-mediated self-organized emergence of collective dynamics, to explain the processes that lead to segmentation.

1. Introduction

The process of development in biological organisms crucially involves the self-organized emergence of spatial patterns [1]. One of the most ubiquitous of such patterns is manifest during somitogenesis, i.e. the formation of somites, which are the modular building blocks of all vertebrate bodies [2–4]. Somites compose bilaterally symmetric segments that are formed in the paraxial, or presomitic mesoderm (PSM) of developing embryos as the body axis itself elongates [5]. Analogous processes have been implicated in the body segmentation of some invertebrates [6, 7]. Although there is great variability across species in terms of the number of somites, the mean size of a somite and the duration over which they are formed, nonetheless a conserved set of features characterizing somitogenesis is seen across these species [8]. A general conceptual model for explaining these core features is provided by the clock and wavefront (CW) framework proposed by Cooke and Zeeman in 1976 [9], that allows the translation of a temporal sequence into a spatial pattern [10]. They assumed the PSM to comprise cellular oscillators (clocks) which are each arrested at their instantaneous state of activity upon encountering a wavefront that moves from the anterior to the posterior of the PSM [11–18]. In order to construct an explicit mechanism embodying the CW framework, we need to disaggregate its components that operate at different length scales, namely, (i) the cellular scale at which oscillations occur, (ii) the inter-cellular scale at which contact-mediated signaling takes place, and (iii) the scale of the PSM across which morphogen gradients form and act as the environment that could modulate the inter-cellular interactions. This resonates with the proposal of Oates [19] to view the CW framework as a three-tier process. In the bottom tier, we observe oscillations at the level of a single cell in the PSM, arising from the periodic expression of clock genes [20–27]. The middle tier describes the mechanism by which the cellular oscillators coordinate their activity with that of their neighbors. This occurs through juxtacrine signaling brought about by interactions between notch

receptors and delta ligands [23, 28–39]. Indeed, several earlier models have explored the role of notch-delta coupling in bringing about robust synchronization between the oscillators [40–45]. Finally, processes that bring about the slowing down (and eventual termination) of the oscillations [20, 33, 46], and the subsequent differentiation of the cells into rostral and caudal halves of the somites [47], constitute the top tier.

In this paper we propose a model that integrates these different length scales by investigating genetic oscillators interacting via notch-delta coupling whose strength is modulated in a position-dependent manner due to a morphogen concentration gradient along the anteroposterior (AP) axis of the PSM. This provides an unified framework for explaining the dynamical transitions observed during somitogenesis. As the PSM expands along the AP axis through the addition of new cells at the tail [5], it is reasonable to restrict our attention to the process of somitogenesis taking place along a one-dimensional array of coupled cells in the PSM. From the perspective of our modeling which explicitly investigates the role of morphogen gradient in coordinating somite formation, the array of cells is considered to be aligned along the AP axis, as the various morphogens that are expressed along the PSM are known to form concentration gradients along this axis [48]. These primarily include molecules belonging to the fibroblast growth factor (FGF) [49, 50], retinoic acid (RA) [51, 52] and wingless/integrated (Wnt) families [53–55]. Even though the role of gradients on the overall dynamics has been explored [56–59], there is to date no consensus as to the explicit mechanism through which they contribute to somite formation. Our model demonstrates that if the morphogen gradient is considered to regulate the impact of the NICD on the expression of the clock genes, it can lead to qualitatively different kinds of dynamics along the PSM in a threshold-dependent manner (figure 1(a)). The dynamical evolution of our model culminates with the emergence of somites, each comprising two cells, that resemble the empirically observed segments that occur towards the tail end of the mesoderm [60, 61]. Unlike the conventional boundary-organized pattern formation paradigm [62], here the morphogen gradient does not determine the cell fate so much as affect the interaction between neighboring cells that lead to dynamical transitions similar to those observed in somitogenesis. This is in contrast to previous work where spatial heterogeneity introduced by the morphogen gradient is incorporated through variations in the autonomous oscillatory behavior of individual cells [63, 64]. Also, while it has been suggested that the mechanical deformations that the tissue undergoes during development could play a role in somitogenesis [65, 66], our work shows that its broad features can be explained exclusively by the interactions between cells and the morphogen signal. While earlier studies have reproduced the different spatio-temporal patterns that arise over the course of somite formation [67–69], the significance of the model presented here centers around demonstrating that morphogen gradients may play a crucial role in regulating inter-cellular notch-delta mediated interactions, whose role in somitogenesis has been established experimentally [70, 71]. Thus, our results help address an open question as to how morphogen gradients influence the collective dynamics of the cellular oscillators by differentially modulating the inter-cellular coupling both in space and time.

2. Methods

2.1. Modeling genetic oscillators interacting via notch-delta coupling

Several experiments have established that the cells in the PSM have 'clock' genes whose expression levels oscillate [20–25, 27]. In our model, we consider a generic two component genetic oscillator comprising an activator gene (x), which upregulates its own expression, as well as that of an inhibitor gene (y), which suppresses the expression of the activator gene [72]. The dynamics of this two-component oscillator can be expressed in terms of a pair of rate equations describing the change in concentrations of the protein products X and Y of genes x and y, respectively (which, in the case of zebrafish, can be identified with the *her1* and *her7* genes [19, 40]). The model parameters are chosen such that X and Y exhibit limit cycle oscillations (see supplementary information, figure S1 (https://stacks.iop.org/PB/19/016001/mmedia)).

As the communication between cells in the PSM is crucial in mediating their collective behavior during somitogenesis, we couple the dynamics of the clock genes of neighboring cells. Experiments have established the role of the notch-delta juxtacrine signaling pathway in mediating the interaction between cells that are in physical contact with each other [23, 28–37]. Such a receptor-ligand based mechanism is crucial for allowing communication between cells during processes such as somitogenesis, as gene products (proteins or mRNA) are too large to be transported across the cellular membrane, thereby preventing direct interaction between cells via diffusion [73]. In general, each cell has both notch receptors as well as delta ligands on their surface. A notch receptor on cell i which is bound to a delta ligand belonging to a neighboring cell j (i.e. *trans* binding) leads to the cleavage of NICD that will act as TF for downstream genes in cell i [74, 75]. In our model, following references [40, 42], NICD upregulates the expression of both the clock genes, while the gene products X, Y suppress the production of delta ligands by the cell. We describe the notch-delta signaling mechanism through the coupled dynamics of (i) the free (unbound) notch receptor concentration

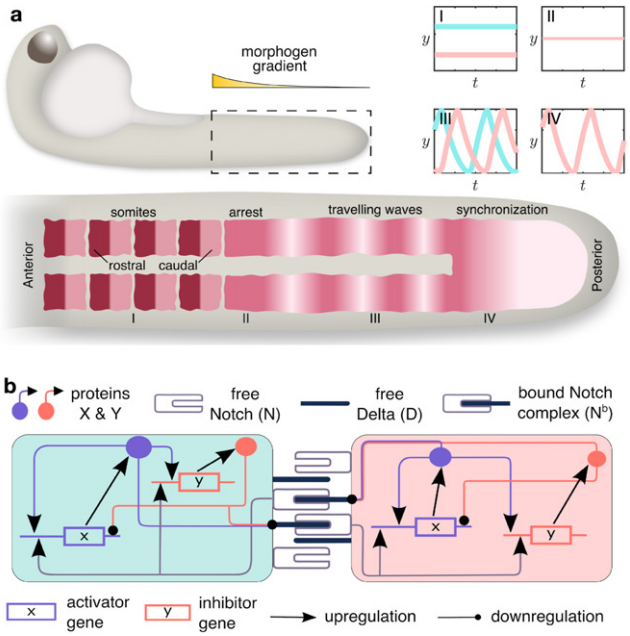

Figure 1. The key dynamical features of somitogenesis (top) that are reproduced in our mathematical model (bottom). (a) Schematic diagram depicting the zebrafish PSM and the dynamical states exhibited by the cells over the course of somitogenesis. The box outlined with broken lines represents the posterior region which exhibits a spatial gradient in morphogen concentration, represented by the exponentially varying profile shown above the box. The dynamics of the cells at the tail (region IV) are characterized by exact synchronization (ES) of the periodic variation in gene expression. As the cells move towards the anterior, they first exhibit travelling waves of gene expression (III), followed by arrest of the oscillations (II). Eventually the cells differentiate (I) into alternating bands corresponding to rostral and caudal halves of the mature somites. The figures in the insets at the right display typical time series in each of the regimes I–IV of the inhibitor gene expression for two neighboring cells coupled to each other. (b) Schematic diagram describing the interaction between two cells via notch-delta coupling. In general, each cell has notch receptors, as well as, delta ligands that bind to them. The *cis* form of the binding leads to the loss of receptors and ligands without resulting in any downstream signaling, whereas *trans* notch-delta binding gives rise to cleavage of the notch intra-cellular domain (NICD). The latter acts as a transcription factor (TF) for the downstream activator (x) and inhibitor (y) genes which are the essential constituents of each cellular oscillator. The proteins X and Y resulting from the expression of these genes, in turn, downregulate the production of delta ligands (the repression being indicated by arrows with circular heads).

(N), (ii) the free delta ligand (D) and (iii) the NICD which is released as a result of *trans* binding (N^b) (see the schematic diagram shown in the supplementary information, figure S3). Thus, the dynamics of a cell i coupled to its neighbors through notch-delta signaling is described by the following set of equations:

$$\frac{dX_i}{dt} = \frac{a + bX_i^2 + fN_i^b}{1 + X_i^2 + Y_i^2 + N_i^b} - cX_i, \tag{1}$$

$$\frac{dY_i}{dt} = \frac{eX_i^2 + g_i(t)N_i^b}{1 + X_i^2 + N_i^b} - Y_i, \tag{2}$$

$$\frac{dN_i}{dt} = \beta^N - \gamma N_i - k^{\rm cis} D_i N_i - k^{\rm tr} D^{\rm tr} N_i, \tag{3}$$

$$\frac{dN_i^b}{dt} = k^{\rm tr} D^{\rm tr} N_i - \mu N_i^b, \tag{4}$$

$$\frac{dD_i}{dt} = \frac{\beta^D}{1 + h\,(X_i^2 + Y_i^2)} - \gamma D_i - k^{\rm cis} D_i N_i - k^{\rm tr} D_i N^{\rm tr}. \tag{5}$$

Here the terms $D^{\rm tr}$ and $N^{\rm tr}$ are the mean values of D_j and N_j over all neighboring cells j to which i is coupled through *trans*-binding. The functional form chosen for the terms corresponding to binding interactions in equations (1), (2), and (5) represent the fact that the TFs compete with each other to bind to the same site in the regulatory regions of the genes coding for X, Y and D, respectively. While the values of the model parameters can, in general, vary across cells, we restrict our attention to the spatio-temporal variation of the coupling parameter g (subscripted with the cell index in equation (2)), which determines the strength of upregulation of y by the NICD (N^b). This allows us to investigate the role of spatial heterogeneity imposed by the gradient of morphogen concentration along the AP axis of the PSM. For the simulations reported here we have considered the case $k^{\rm tr} = k^{\rm cis} = 1$. We note that our results are qualitatively unchanged in the absence of *cis*-inhibition (see supplementary information, figure S4).

2.2. Morphogen gradients in the PSM

It is known that the morphogens RA, Wnt and FGF are differentially expressed along the PSM, exhibiting monotonically varying concentration gradients having peaks at the posterior (for FGF and Wnt) or anterior (for RA) ends [54, 77, 78]. Experiments on several vertebrate species have shown that high concentrations of RA initiate differentiation, while increased levels of Wnt and FGF, which are known to promote sustained oscillations in the expression

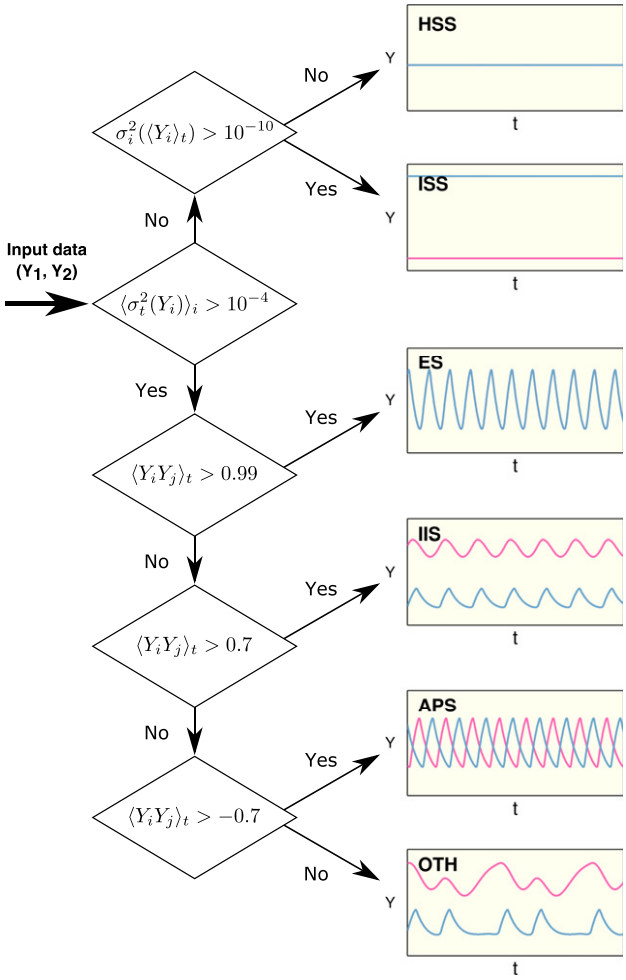

Figure 2. Flow chart illustrating the algorithm used to classify the collective dynamical patterns obtained for a system of two coupled oscillators. To distinguish between oscillating and non-oscillating patterns, we use $\langle \sigma_t^2(Y_i)\rangle_i$ which is the mean temporal variance of the time series of Y, the concentration of the protein product of gene y, calculated over the two oscillators. To determine whether the steady states (SS) that the oscillators have reached are the same (corresponding to HSS) or different (corresponding to ISS), we compute the variance of the mean values for the two time series, $\sigma_i^2(\langle Y_i\rangle_t)$. To distinguish between the oscillating patterns, we use the equal time linear correlation between the two time series, $\langle Y_iY_j\rangle_t$. The classification is robust with respect to small changes in the values of the thresholds, which are displayed in the figure.

of the clock genes, impede the formation of mature somites [49, 52, 79, 80]. Note that some aspects of the roles played by Wnt and FGF are already accounted for in the local dynamics of our model, where each cell is capable of autonomous robust oscillations. As our primary goal is to explicate the mechanisms driving termination of oscillatory activity followed by cellular differentiation, we focus on the role of RA on the collective dynamics of cells in the PSM. We incorporate the effect of this morphogen in the spatial variation of the coupling parameter g which is assumed to exponentially decay from the anterior to the posterior end of the domain. Such a profile will naturally arise if the morphogen diffuses from a source located at the anterior and is degraded at a constant rate across space [81–83]. The regulation of the notch-mediated interaction can come about by the binding of a morphogen molecule to a cell surface receptor leading to (either directly or indirectly) the expression of molecules that aid NICD or its downstream effector to bind more strongly to the promoter site of gene Y. This contrasts with earlier studies (e.g. see reference [84]) that have assumed the morphogen to regulate the gene expressing notch, which would affect expression of both X and Y (instead of selectively affecting only Y as in the present model).

2.3. Dynamical evolution of the morphogen gradient

Our model focuses on the behavior of a contiguous segment of cells of length ℓ in the PSM with a morphogen source located at its anterior. If the strength of the source is constant in time, it would have resulted in the gradient becoming progressively less steep as the PSM expands. This dilution is countered by the net increase in the strength of the source through the secretion of morphogen by the newly matured somites (see supplementary information, figure S6). Thus, as the PSM expands due to addition of cells at the posterior tail, we can view the segment under consideration as effectively flowing up a morphogen gradient along the AP axis [19]. We choose a segment

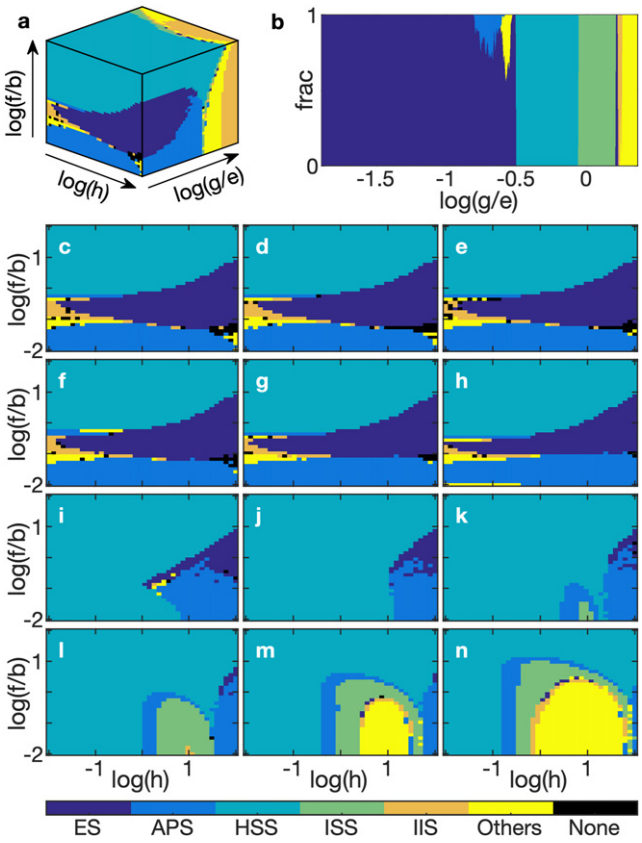

Figure 3. Transitions between patterns representing different stages in somitogenesis seen in the collective dynamics of a pair of cells on varying the parameters governing the strength of notch-delta coupling in our model. (a) Schematic diagram of the three-dimensional space spanned by the coupling parameters (f, g, h), scaled by the relevant kinetic parameters of the individual oscillators. Note the logarithmic scale used for the ranges of the parameters. (b) The variation with g of the relative frequency of occurrence of patterns belonging to each of six distinct categories, viz, ES, APS, HSS, ISS, inhomogeneous in-phase synchronization and other dynamical patterns (Others) ('none' refers to those regions of parameter space in which no single pattern dominates). The values of the parameters f/b and h are fixed at 0.25 and 4, respectively. (c)–(n) The most commonly occurring dynamical patterns (i.e. obtained for $>50\%$ of all initial conditions used) that are seen for different values of f/b and h (varying over four order of magnitude) for 12 equally spaced values of $\log(g/e)$ between -1.89 (panel (c)) and 0.36 (panel (n)). While HSS is the most common pattern seen over this range of parameter values, focusing on how the occurrence frequency of ES varies with f, g, h indicates where a transition from synchronization to time-invariant behavior may be achieved. In all cases, initial values of the dynamical variables for each cell are independently and identically distributed uniformly over the unit interval. Unless mentioned otherwise, the following parameter values have been used for all model simulations: $a = 16.0$, $b = 200.0$, $c = 20.0$, $e = 10.0$, $\beta^N = 5.0$, $\beta^D = 100.0$, $\gamma = 1.0$, $k^{\mathrm{tr}} = 1.0$, $k^{\mathrm{cis}} = 1.0$ and $\mu = 1.0$.

of N cells with a spatial extent ℓ that is initially located $(t = 0)$ at the posterior end of the PSM, i.e. at the lower end of the gradient. Its evolution is followed for a duration T, the time required for the array of cells to move across the entire spatial extent of the morphogen gradient considered here. Thus, it determines the rate at which cells move along the gradient, which in turn is related to the rate at which the PSM expands by cell division at its posterior end. As mentioned above, the effect of the varying morphogen concentration on the dynamics of the cells is introduced via the coupling parameter g. Specifically, we assume that the value of g at each site is proportional to the corresponding morphogen concentration, yielding an exponentially varying gradient of g across the AP axis: $g_i(t) = g_{\mathrm{min}} \exp\left(\lambda_{\mathrm{g}} x_i(t)\right)$. The steepness of the gradient is quantified by λ_{g}, which is a function of T, as well as g_{max} and g_{min}, which are the values of g at the anterior and posterior ends of the PSM, respectively, viz, $\lambda_{\mathrm{g}} = \ln(g_{\mathrm{max}}/g_{\mathrm{min}})/T$. We assume that the effective flow of the segment of cells along the AP axis occurs at an uniform rate. This can be taken to be unity without loss of generality by appropriate choice of time unit. Thus, the instantaneous position $x_i(t)$ along the gradient of the ith cell in the segment is given by $x_i(t) = t + (\ell/N)(i - 1)$, with the initial condition as $x_1(t = 0) = 0$.

3. Results

In our simulations, we have considered the PSM to comprise cells, each of which exhibits oscillating gene expression. We assume a minimal model for the genetic oscillator consisting of two clock genes, one activatory and the other inhibitory, whose products correspond to fate determining proteins (see Methods). The oscillations of neighboring cells influence each other through notch-delta inter-cellular coupling (figure 1(b)). We have explicitly verified that

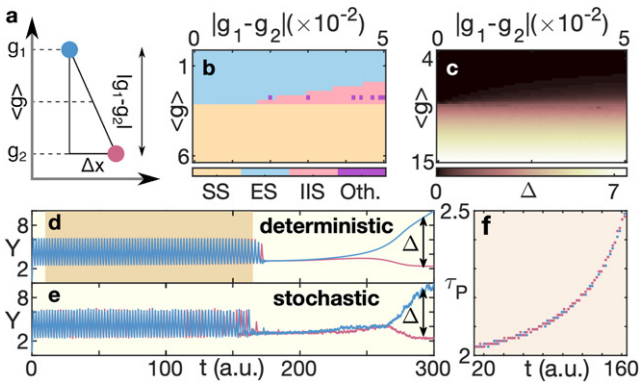

Figure 4. Incorporating a morphogen gradient by varying the notch-delta coupling parameter g of adjacent oscillators reproduces the temporal sequence of patterns observed during somitogenesis. (a) Schematic representation of the spatial variation of g, resulting from the different concentrations of a morphogen sensed by neighboring cells, which are separated by a distance Δx in space. The steepness of the gradient is quantified by $|g_1 - g_2|$, the difference in the values $g_{1,2}$ for the two oscillators, while their location on the gradient is determined by the mean $\langle g \rangle$. (b) The most commonly occurring dynamical patterns (i.e. obtained for >50% of all initial conditions used) on varying $|g_1 - g_2|$ and $\langle g \rangle$. The states of the adjacent cells, characterized by the protein concentration Y, converge to fixed points $Y_{1,2}$ in the SS region. (c) The difference between the SS concentrations of the adjacent cells, $\Delta = |Y_1 - Y_2|$, increases with $\langle g \rangle$ as one effectively moves up the morphogen gradient, while being relatively unaffected by the steepness $|g_1 - g_2|$. (d)–(f) The dynamical consequences of a morphogen gradient with an exponentially varying concentration profile. (d) As a pair of coupled cells gradually move upstream of the gradient, resulting in an increase of $g_{1,2}$ over time t, their collective behavior (represented by Y) converges from initially synchronized oscillations (ES) to an inhomogeneous steady state (ISS, characterized by finite values of Δ) at long times. These transitions are robust with respect to stochastic fluctuations (as shown in panel (e)). The changes occurring in the system during the transition from oscillations to SS behavior (shaded region) can be quantitatively investigated by focusing on how the period τ_p of the oscillations changes over time. (f) As cells move upstream of the morphogen gradient (corresponding to a progression from posterior to anterior regions in the PSM), the model displays an increase in time period τ_p. This is consistent with a key experimental observation, viz, slowing of oscillations as cells approach the anterior end of the PSM, during somitogenesis. The coupling parameters are $f = 50$, $h = 4$, $g_{max} = 15$ and $g_{min} = 0.5$, with $\Delta x = 3$ arb. units.

incorporating delay in the contact mediated signaling does not alter our results qualitatively (see supplementary information, figure S5).

3.1. Dynamics of a pair of coupled cells

In the simplest setting, namely, a pair of adjacent cells, which allows us to investigate the effect of coupling on the collective dynamics, the system can exhibit a wide range of spatio-temporal patterns. These can be classified systematically through the use of quantitative measures (see figure 2). We focus on the patterns that can be immediately interpreted in the context of somitogenesis: (i) inhomogeneous steady states (ISS), (ii) homogeneous steady states (HSS), (iii) anti-phase synchronization (APS) and (iv) ES (shown schematically as insets of figure 1(a)). The range of values of the coupling-related parameters f, g and h over which these patterns are observed in a pair of coupled cells are shown in figure 3. The parameters f and g govern the strength with which the NICD (N^b) regulates the activatory and inhibitory clock genes, respectively, while h is related to the intensity of repression of the delta ligand (D) by each of the clock genes. As inter-cellular coupling is believed to be responsible for the synchronized activity of cells in the initial stage of somitogenesis [76], we note that the dynamical regime corresponding to ES occurs for low g and intermediate values of f, with the region increasing in size for larger h.

3.2. Morphogen gradient-induced heterogeneity in a pair of coupled cells

Spatial variation in these coupling parameters across the PSM can arise through heterogeneity in the underlying morphogen concentrations. Introducing heterogeneity through the coupling parameter g in the pair of adjacent cells considered earlier (g_1 and g_2 being their respective values), we observe that qualitatively similar spatio-temporal patterns to those observed in figure 3 are obtained. On varying the mean value of the coupling $\langle g \rangle = (g_1 + g_2)/2$, which effectively represents the location of these cells on the PSM, and the steepness of the gradient $|g_1 - g_2|$ (figure 4(a)), the range of $\langle g \rangle$ over which ES is seen (corresponding to the region proximal to the posterior end of the PSM) does not appear to change appreciably on increasing $|g_1 - g_2|$ (figure 4(b)). Above a critical value of $\langle g \rangle$ which is independent of the gradient, the activities of the cells are arrested at Y_1 and Y_2, respectively, with the gap $\Delta = |Y_1 - Y_2|$ becoming larger as we move towards the anterior end, corresponding to increasing $\langle g \rangle$ (figure 4(c)).

As explained in the Methods, over the course of development, the PSM expands through new cells being added to its posterior end, such that the existing cells progressively encounter increasing values of the morphogen concentration. Modeling this time-evolution as an effective flow of the segment of adjacent cells along the gradient in g, we observe that a

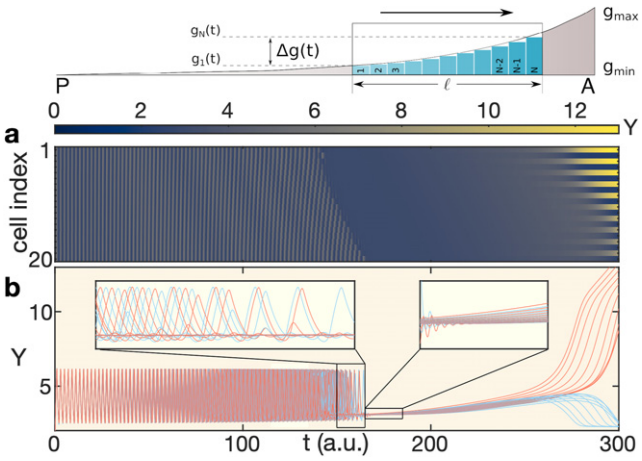

Figure 5. Collective dynamics of a cellular array responding to an exponential gradient of morphogen concentration reproduces the spatio-temporal evolution of PSM activity seen during somitogenesis. The transition from progenitor cells in the posterior (P) to maturity at the anterior (A) of a segment of length ℓ comprising N cells in the PSM viewed as a flow upstream (moving window in the schematic on top) over a period of time T along the exponential profile of the parameter g, decaying from g_{max} to g_{min}, reflecting the morphogen gradient. Different cells in the window sense different morphogen concentrations, whose values change over time. This is incorporated in terms of the time-dependent gradient $\Delta g(t)$, with $g_1(t)$ and $g_N(t)$ being the values of the coupling parameter g at the anterior and posterior ends of the window at time t, respectively. The resulting change in the activity of a segment comprising $N = 20$ coupled cells, as it moves from P to A, is shown in (a). The system initially exhibits synchronized oscillations across the segment but, as a consequence of the gradient, a phase lag develops between adjacent cells (as seen in the time series in panel (b), where odd and even numbered cells are represented using red and blue curves, respectively). This results in a wave-like propagation of the peak expression from the anterior to the posterior end of the segment in each cycle. Subsequently, the oscillations reduce in intensity leading to arrest of the oscillations, a magnified view of the transition being shown in the left inset of panel (b). This is followed by a divergence of the dynamical trajectories followed by the different cells, as shown in the right inset of (b). This gives way to an ISS with adjacent cells attaining different fates characterized by alternating high and low values of the protein concentration Y (cells with odd and even indices on the segment are shown using different colors in panel (b)). Results shown are for parameter values of $g_{max} = 15$, $g_{min}(= g_0) = 0.5$ and $T = 300$ a.u. In all cases, initial values of the dynamical variables for each cell are independently and identically distributed uniformly over the unit interval. We note that NICD concentration at each cell exhibits qualitatively similar dynamics (see supplementary information, figure S10).

transient phase of ES is followed by desynchronization and subsequent attenuation of the oscillations, eventually leading to a separation of the SS of the two cells (figure 4(d); see also supplementary information, figure S7)]. The gap Δ between the SS increases with time, giving rise to a pronounced ISS state. This duration depends sensitively on the steepness of the morphogen concentration gradient (see supplementary information, figure S8). The sequence of dynamical transitions seen in the model are robust with respect to the presence of noise as shown explicitly in figure 4(e) by introducing stochastic fluctuations in the dynamical variables (see also supplementary information, figure S9). Immediately preceding the arrest of periodic activity, we observe that the period τ_P (figure 4(f)) of the oscillations increases with time that is in agreement with experimental observations of somitogenesis [85, 86].

3.3. Dynamics of a cellular array in a growing PSM in presence of a morphogen gradient

Having seen that a pair of contiguous cells can indeed converge to markedly different SS values of their clock gene expressions, we now investigate the generalization to a spatially extended segment of length ℓ in the growing PSM subject to a morphogen gradient (varying from g_{min} to g_{max} as shown schematically above figure 5(a)). As the principal variation of the morphogen concentration occurs along the AP axis of the PSM, we restrict our focus to a one-dimensional array of cells aligned along this axis. As new cells are added to the posterior of the PSM over time, the relative position of the segment of cells under consideration shifts along the morphogen gradient from the posterior to the anterior. We note that had there been a temporally invariant source of morphogen at the anterior, the expansion of the PSM would have resulted in a dilution of the gradient. However, newly matured somites at the anterior end serve as additional sources of the morphogen over time [87–89], thereby ensuring that each cell experiences an exponential increase in the morphogen concentration. This is reproduced in our model by the segment effectively flowing up the morphogen gradient (as discussed in Methods). As shown in figure 5(a), for a range of values of the parameters g_{max}, g_{min} and ℓ, the cells display a short-lived ES pattern, which is followed by the development of a phase lag between adjacent cells (as can be seen in the inset of figure 5(b)). This is analogous to the appearance of a small phase difference between the pair of oscillators described earlier, and manifests as a travelling wave that propagates along the PSM. We note that such a travelling wave of gene expression has indeed been experimentally observed to move through the PSM towards the anterior [19, 24, 54]. As the cells move further up the gradient, the oscillations subside, eventually giving way to a

heterogeneous SS characterized by adjacent cells having alternating high and low clock gene expressions. The gap between these high and low values increases with time to eventually produce a distinctive pattern that resemble the stripes that arise due to polarization of each somite into rostral and caudal halves (as seen for large t in both figures 5(a) and (b)). In this asymptotic SS, the separation between the high and low values for clock gene expression is greater than the amplitude of the oscillations seen at lower values of t. Thus, we can reproduce the entire sequence of dynamical transitions observed in the PSM during somitogenesis through a model incorporating an array of oscillators that interact via notch-delta signaling while 'moving up' a morphogen gradient. We note that, in different organisms, the size of somites vary across the mesoderm, with the ones occurring at the posterior end being smaller [90] and resembling the segments consisting of pairs of cells that arise in our model. We would like to point out that the dynamics resulting from the inter-cellular interactions can yield ISS states having larger spatial periodicities, which suggests a potential for producing larger somites (see supplementary information, figure S11). We also note that introducing additional mechanisms such as lateral induction via jagged receptors [91] or diffusive coupling between cells via gap junctions [67, 69] may allow for variation in the wavelength of the periodic pattern.

4. Discussion

Somitogenesis is seen across all vertebrates, and recent evidence implies that mechanisms underlying it could have analogues even in segmentation of invertebrates, such as arthropods [6, 92]. It would appear that there is an invariant set of mechanisms responsible for this process, that differ only in terms of the specific identities of the contributing molecular players across species. Thus, somitogenesis would in general involve (i) a cellular 'clock', (ii) means by which neighboring clocks communicate, and (iii) a spatial gradient of signaling molecules, which introduces heterogeneity in the interactions between the clocks. We have shown here that incorporating these three elements in a model of a PSM, that grows through the addition of cells at the posterior, reproduces the sequence of invariant dynamical transitions seen in somitogenesis.

While the roles of interacting clocks and that of morphogen gradients have been investigated individually in earlier studies, we provide here a framework to understand how these two work in tandem to give rise to the key features associated with somitogenesis. In particular, our results shed light on the significance of the steepness of the morphogen gradient. For instance, we may consider the consequences of a reduction in the steepness leading to a linear profile for the morphogen gradient which can arise, for example, when the degradation rate is negligible. On replacing the exponential morphogen gradient in our model with a linear one, we observe a very long-lived transient state before the system converges to an inhomogeneous SS. This therefore suggests that exponential gradients allow relatively rapid switching between qualitatively distinct dynamical regimes. Hence, by varying the steepness of the RA gradient experimentally it should be possible to determine how the time required for maturation changes as a consequence. This is especially true in the case of the time interval between cessation of oscillations and the polarization of the somites. As inter-cellular coupling is also known to regulate the period of the segmentation clock [93], it is possible that introducing other morphogen gradients, that influence the strength of the coupling, can explain variations in the rate at which somites form over time. The broad features observed here can be reproduced in two-dimensional cellular arrays with anisotropic inter-cellular coupling (see supplementary information, figure S12). Furthermore, the core assumption of our model, namely that notch-delta coupling plays a crucial role in regulating somitogenesis in the presence of a morphogen gradient can be probed in experimental systems where notch signaling has been arrested. It would also be intriguing to experimentally test whether the morphogen affects the expression of the patterning genes selectively, which would be the case if morphogen gradient acts on the coupling of the notch signaling to the patterning gene expression dynamics (as has been assumed here) rather than on production of notch. Future research involving incorporation of additional details in the model presented here may provide answers to several challenges that explanations of somitogenesis based on the clock-and-wavefront mechanism have faced [94].

Acknowledgments

We would like to thank Krishnan Iyer, Jose Negrete Jr, Shubha Tole and Vikas Trivedi for valuable suggestions. The authors would like to acknowledge discussions during the ICTP/ICTS Winter Schools on Quantitative Systems Biology (ICTP/smr2879, ICTS/qsb2019/12). SNM has been supported by the IMSc Complex Systems Project (12th Plan), and the Center of Excellence in Complex Systems and Data Science, both funded by the Department of Atomic Energy, Government of India. The simulations and computations required for this work were supported by High Performance Computing facility (Nandadevi and Satpura) of The Institute of Mathematical Sciences, which is partially funded by Department of Science and Technology, Government of India.

Data availability statement

All data that support the findings of this study are included within the article (and any supplementary files).

ORCID iDs

Chandrashekar Kuyyamudi https://orcid.org/0000-0001-8579-4871
Shakti N Menon https://orcid.org/0000-0001-5307-2153
Sitabhra Sinha https://orcid.org/0000-0002-3004-1079

References

[1] Koch A J and Meinhardt H 1994 Biological pattern formation: from basic mechanisms to complex structures *Rev. Mod. Phys.* **66** 1481–507
[2] Dequéant M-L and Pourquié O 2008 Segmental patterning of the vertebrate embryonic axis *Nat. Rev. Genet.* **9** 370
[3] Gomez C, Özbudak E M, Wunderlich J, Baumann D, Lewis J and Pourquié O 2008 Control of segment number in vertebrate embryos *Nature* **454** 335
[4] Vonk F J and Richardson M K 2008 Developmental biology: serpent clocks tick faster *Nature* **454** 282
[5] Gilbert S F 2013 *Developmental Biology* (Sunderland, MA: Sinauer)
[6] Stollewerk A, Schoppmeier M and Damen W G M 2003 Involvement of notch and delta genes in spider segmentation *Nature* **423** 863
[7] Sarrazin A F, Peel A D and Averof M 2012 A segmentation clock with two-segment periodicity in insects *Science* **336** 338–41
[8] Pourquié O and Tam P P L 2001 A nomenclature for prospective somites and phases of cyclic gene expression in the presomitic mesoderm *Dev. Cell* **1** 619–20
[9] Cooke J and Zeeman E C 1976 A clock and wavefront model for control of the number of repeated structures during animal morphogenesis *J. Theor. Biol.* **58** 455–76
[10] Pourquié O 2003 The segmentation clock: converting embryonic time into spatial pattern *Science* **301** 328–30
[11] Baker R E, Schnell S and Maini P K 2006 A clock and wavefront mechanism for somite formation *Dev. Biol.* **293** 116–26
[12] Santillán M and Mackey M C 2008 A proposed mechanism for the interaction of the segmentation clock and the determination front in somitogenesis *PLoS One* **3** e1561
[13] Nagahara H, Ma Y, Takenaka Y, Kageyama R and Yoshikawa K 2009 Spatiotemporal pattern in somitogenesis: a non-turing scenario with wave propagation *Phys. Rev.* E **80** 021906
[14] Hester S D, Belmonte J M, Gens J S, Clendenon S G and Glazier J A 2011 A multi-cell, multi-scale model of vertebrate segmentation and somite formation *PLoS Comput. Biol.* **7** e1002155
[15] Ares S, Morelli L G, Jörg D J, Oates A C and Jülicher F 2012 Collective modes of coupled phase oscillators with delayed coupling *Phys. Rev. Lett.* **108** 204101
[16] Murray P J, Maini P K and Baker R E 2013 Modelling delta-notch perturbations during zebrafish somitogenesis *Dev. Biol.* **373** 407–21
[17] Jörg D J, Morelli L G, Ares S and Jülicher F 2014 Synchronization dynamics in the presence of coupling delays and phase shifts *Phys. Rev. Lett.* **112** 174101
[18] Wiedermann G, Bone R A, Silva J C, Bjorklund M, Murray P J and Dale J K 2015 A balance of positive and negative regulators determines the pace of the segmentation clock *eLife* **4** e05842
[19] Oates A C, Morelli L G and Ares S 2012 Patterning embryos with oscillations: structure, function and dynamics of the vertebrate segmentation clock *Development* **139** 625–39
[20] Palmeirim I, Henrique D, Ish-Horowicz D and Pourquié O 1997 Avian hairy gene expression identifies a molecular clock linked to vertebrate segmentation and somitogenesis *Cell* **91** 639–48
[21] Dale K J and Pourquié O 2000 A clock-work somite *Bioessays* **22** 72–83
[22] Saga Y and Takeda H 2001 The making of the somite: molecular events in vertebrate segmentation *Nat. Rev. Genet.* **2** 835
[23] Maroto M, Dale J K, Dequeant M-L, Petit A-C and Pourquié O 2005 Synchronised cycling gene oscillations in presomitic mesoderm cells require cell-cell contact *Int. J. Dev. Biol.* **49** 309–15
[24] Masamizu Y, Ohtsuka T, Takashima Y, Nagahara H, Takenaka Y, Yoshikawa K, Okamura H and Kageyama R 2006 Real-time imaging of the somite segmentation clock: revelation of unstable oscillators in the individual presomitic mesoderm cells *Proc. Natl Acad. Sci.* **103** 1313–8
[25] Riedel-Kruse I H, Mu¨ller C and Oates A C 2007 Synchrony dynamics during initiation, failure, and rescue of the segmentation clock *Science* **317** 1911–5
[26] Schröter C *et al* 2012 Topology and dynamics of the zebrafish segmentation clock core circuit *PLoS Biol* **10** e1001364
[27] Webb A B, Lengyel I M, Jörg D J, Valentin G, Jülicher F, Morelli L G and Oates A C 2016 Persistence, period and precision of autonomous cellular oscillators from the zebrafish segmentation clock *eLife* **5** e08438
[28] Jiang Y-J, Smithers L and Lewis J 1998 Vertebrate segmentation: the clock is linked to notch signalling *Curr. Biol.* **8** R868–71
[29] Ferjentsik Z, Hayashi S, Dale J K, Bessho Y, Herreman A, De Strooper B, del Monte G, de la Pompa J L and Maroto M 2009 Notch is a critical component of the mouse somitogenesis oscillator and is essential for the formation of the somites *PLoS Genet.* **5** e1000662
[30] Hubaud A and Pourquié O 2014 Signalling dynamics in vertebrate segmentation *Nat. Rev. Mol. Cell. Biol.* **15** 709–21
[31] Conlon R A, Reaume A G and Rossant J 1995 Notch1 is required for the coordinate segmentation of somites *Development* **121** 1533–45
[32] Pourquié O 1999 Notch around the clock *Curr. Opin. Genet. Dev.* **9** 559–65
[33] Jiang Y-J, Aerne B L, Smithers L, Haddon C, Ish-Horowicz D and Lewis J 2000 Notch signalling and the synchronization of the somite segmentation clock *Nature* **408** 475
[34] Lai E C 2004 Notch signaling: control of cell communication and cell fate *Development* **131** 965–73
[35] Huppert S S, Ilagan M X G, De Strooper B and Kopan R 2005 Analysis of notch function in presomitic mesoderm suggests a γ-secretase-independent role for presenilins in somite differentiation *Dev. Cell* **8** 677–88
[36] Mara A and Holley S A 2007 Oscillators and the emergence of tissue organization during zebrafish somitogenesis *Trends Cell Biol.* **17** 593–9
[37] Kageyama R, Masamizu Y and Niwa Y 2007 Oscillator mechanism of notch pathway in the segmentation clock *Dev. Dyn.* **236** 1403–9
[38] Sprinzak D, Lakhanpal A, LeBon L, Santat L A, Fontes M E, Anderson G A, Garcia-Ojalvo J and Elowitz M B 2010 Cis-interactions between notch and delta generate mutually exclusive signalling states *Nature* **465** 86
[39] Sprinzak D, Lakhanpal A, LeBon L, Garcia-Ojalvo J and Elowitz M B 2011 Mutual inactivation of notch receptors and ligands facilitates developmental patterning *PLoS Comput. Biol.* **7** e1002069
[40] Lewis J 2003 Autoinhibition with transcriptional delay *Curr. Biol.* **13** 1398–408

[41] Giudicelli F and Lewis J 2004 The vertebrate segmentation clock *Curr. Opin. Genet. Dev.* **14** 407–14

[42] Horikawa K, Ishimatsu K, Yoshimoto E, Kondo S and Takeda H 2006 Noise-resistant and synchronized oscillation of the segmentation clock *Nature* **441** 719

[43] Giudicelli F, Özbudak E M, Wright G J and Lewis J 2007 Setting the tempo in development: an investigation of the zebrafish somite clock mechanism *PLoS Biol.* **5** e150

[44] Tiedemann H B, Schneltzer E, Zeiser S, Hoesel B, Beckers J, Przemeck G K H and de Angelis M H 2012 From dynamic expression patterns to boundary formation in the presomitic mesoderm *PLoS Comput. Biol.* **8** e1002586

[45] Tiedemann H B, Schneltzer E, Zeiser S, Wurst W, Beckers J, Przemeck G K H, de Angelis M H and Thieffry D 2014 Fast synchronization of ultradian oscillators controlled by delta-notch signaling with cis-inhibition *PLoS Comput. Biol.* **10** e1003843

[46] McGrew M J and Pourquié O 1998 Somitogenesis: segmenting a vertebrate *Curr. Opin. Genet. Dev.* **8** 487–93

[47] Oginuma M, Takahashi Y, Kitajima S, Kiso M, Kanno J, Kimura A and Saga Y 2010 The oscillation of notch activation, but not its boundary, is required for somite border formation and rostral-caudal patterning within a somite *Development* **137** 1515–22

[48] Gibb S, Maroto M and Dale J K 2010 The segmentation clock mechanism moves up a notch *Trends Cell Biol.* **20** 593–600

[49] Dubrulle J, McGrew M J and Pourquié O 2001 FGF signaling controls somite boundary position and regulates segmentation clock control of spatiotemporal Hox gene activation *Cell* **106** 219–32

[50] Dubrulle J and Pourquié O 2004 fgf8 mRNA decay establishes a gradient that couples axial elongation to patterning in the vertebrate embryo *Nature* **427** 419–22

[51] Dubrulle J and Pourquieé O 2004 Coupling segmentation to axis formation *Development* **131** 5783–93

[52] Vermot J and Pourquié O 2005 Retinoic acid coordinates somitogenesis and left-right patterning in vertebrate embryos *Nature* **435** 215

[53] Aulehla A 2004 Segmentation in vertebrates: clock and gradient finally joined *Genes Dev.* **18** 2060–7

[54] Aulehla A, Wiegraebe W, Baubet V, Wahl M B, Deng C, Taketo M, Lewandoski M and Pourquié O 2008 A β-catenin gradient links the clock and wavefront systems in mouse embryo segmentation *Nat. Cell Biol.* **10** 186

[55] Bajard L, Morelli L G, Ares S, Pécréaux J, Jülicher F and Oates A C 2014 Wnt-regulated dynamics of positional information in zebrafish somitogenesis *Development* **141** 1381–91

[56] Goldbeter A, Gonze D and Pourquié O 2007 Sharp developmental thresholds defined through bistability by antagonistic gradients of retinoic acid and fgf signaling *Dev. Dyn.* **236** 1495–508

[57] Goldbeter A and Pourquié O 2008 Modeling the segmentation clock as a network of coupled oscillations in the notch, Wnt and FGF signaling pathways *J. Theor. Biol.* **252** 574–85

[58] Mazzitello K I, Arizmendi C M and Hentschel H G E 2008 Converting genetic network oscillations into somite spatial patterns *Phys. Rev.* E **78** 021906

[59] Jörg D J, Oates A C and Jülicher F 2016 Sequential pattern formation governed by signaling gradients *Phys. Biol.* **13** 05LT03

[60] Youn B W, Keller R E and Malacinski G M 1980 An atlas of notochord and somite morphogenesis in several anuran and urodelean amphibians *Development* **59** 223–47

[61] Tlili S *et al* 2019 Shaping the zebrafish myotome by intertissue friction and active stress *Proc. Natl Acad. Sci.* **116** 25430–9

[62] Lander A D 2011 Pattern, growth, and control *Cell* **144** 955–69

[63] Murray P J, Maini P K and Baker R E 2011 The clock and wavefront model revisited *J. Theor. Biol.* **283** 227–38

[64] Tomka T, Iber D and Boareto M 2018 Travelling waves in somitogenesis: collective cellular properties emerge from time-delayed juxtacrine oscillation coupling *Prog. Biophys. Mol. Biol.* **137** 76–87

[65] Adhyapok P, Piatkowska A M, Norman M J, Clendenon S G, Stern C D and Belmonte J A and Belmonte J M 2021 A mechanical model of early somite segmentation *iScience* **24** 102317

[66] Narayanan R, Mendieta-Serrano M A and Saunders T E 2021 The role of cellular active stresses in shaping the zebrafish body axis *Curr. Opin. Cell Biol.* **73** 69–77

[67] Meinhardt H 1982 *Models of Biological Pattern Formation* (London: Academic)

[68] François P, Hakim V and Siggia E D 2007 Deriving structure from evolution: metazoan segmentation *Mol. Syst. Biol.* **3** 154

[69] Cotterell J, Robert-Moreno A and Sharpe J 2015 A local, self-organizing reaction-diffusion model can explain somite patterning in embryos *Cell Syst.* **1** 257–69

[70] Wahi K, Bochter M S and Cole S E 2016 The many roles of notch signaling during vertebrate somitogenesis *Semin. Cell Dev. Biol.* **49** 68–75

[71] Liao B-K and Oates A C 2017 Delta-notch signalling in segmentation *Arthropod Struct. Dev.* **46** 429–47

[72] Guantes R and Poyatos J F 2006 Dynamical principles of two-component genetic oscillators *PLoS Comput. Biol.* **2** e30

[73] Goodenough D A and Paul D L 2009 Gap junctions *Cold Spring Harbor Perspect. Biol.* **1** a002576

[74] Takke C and Campos-Ortega J A 1999 her1, a zebrafish pair-rule like gene, acts downstream of notch signalling to control somite development *Development* **126** 3005–14

[75] Oates A C and Ho R K 2002 Hairy/E(spl)-related(Her) genes are central components of the segmentation oscillator and display redundancy with the delta/notch signaling pathway in the formation of anterior segmental boundaries in the zebrafish *Development* **129** 2929–46

[76] Maroto M, Dale J K, Dequeant M-L, Petit A-C and Pourquie O 2005 Synchronised cycling gene oscillations in presomitic mesoderm cells require cell-cell contact *Int. J. Dev. Biol.* **49** 309–15

[77] Gurdon J B and Bourillot P-Y 2001 Morphogen gradient interpretation *Nature* **413** 797

[78] Aulehla A and Pourquié O 2010 Signaling gradients during paraxial mesoderm development *Cold Spring Harbor Perspect. Biol.* **2** a000869

[79] Sawada A, Shinya M, Jiang Y-J, Kawakami A, Kuroiwa A and Takeda H 2001 Fgf/MAPK signalling is a crucial positional cue in somite boundary formation *Development* **128** 4873–80

[80] Moreno T A and Kintner C 2004 Regulation of segmental patterning by retinoic acid signaling during xenopus somitogenesis *Dev. Cell* **6** 205–18

[81] Lander A D, Nie Q and Wan F Y M 2002 Do morphogen gradients arise by diffusion? *Dev. Cell* **2** 785–96

[82] Bergmann S, Sandler O, Sberro H, Shnider S, Schejter E, Shilo B-Z and Barkai N 2007 Pre-steady-state decoding of the bicoid morphogen gradient *PLoS Biol.* **5** 1–11

[83] Barkai N and Shilo B-Z 2009 Robust generation and decoding of morphogen gradients *Cold Spring Harbor Perspect. Biol.* **1** a001990

[84] Hubaud A, Regev I, Mahadevan L and Pourquié O 2017 Excitable dynamics and Yap-dependent mechanical cues drive the segmentation clock *Cell* **171** 668–82

[85] Delaune E A, François P, Shih N P and Amacher S L 2012 Single-cell-resolution imaging of the impact of notch signaling and mitosis on segmentation clock dynamics *Dev. Cell* **23** 995–1005

[86] Shih N P, François P, Delaune E A and Amacher S L 2015 Dynamics of the slowing segmentation clock reveal alternating two-segment periodicity *Development* **142** 1785–93

[87] del Corral R D, Olivera-Martinez I, Goriely A, Gale E, Maden M and Storey K 2003 Opposing FGF and retinoid

pathways control ventral neural pattern, neuronal differentiation, and segmentation during body axis extension *Neuron* **40** 65–79
[88] del Corral R D and Storey K G 2004 Opposing FGF and retinoid pathways: a signalling switch that controls differentiation and patterning onset in the extending vertebrate body axis *Bioessays* **26** 857–69
[89] Rhinn M and Dollé P 2012 Retinoic acid signalling during development *Development* **139** 843–58
[90] Schröter C, Herrgen L, Cardona A, Brouhard G J, Feldman B and Oates A C 2008 Dynamics of zebrafish somitogenesis *Dev. Dyn.* **237** 545–53
[91] Hadjivasiliou Z, Hunter G L and Baum B 2016 A new mechanism for spatial pattern formation via lateral and protrusion-mediated lateral signalling *J. R. Soc. Interface* **13** 20160484
[92] Clark E, Peel A D and Akam M 2019 Arthropod segmentation *Development* **146** dev170480
[93] Herrgen L, Ares S, Morelli L G, Schröter C, Jülicher F and Oates A C 2010 Intercellular coupling regulates the period of the segmentation clock *Curr. Biol.* **20** 1244–53
[94] Stern C D and Piatkowska A M 2015 Multiple roles of timing in somite formation *Semin. Cell Dev. Biol.* **42** 134–9